

# あらせ衛星/MGF センサにおける人工衛星起因の直流成分磁場ノイズ (1) Tsyganenko 89 モデルを用いた評価

山本 和弘<sup>\*1</sup>, 生松 聡<sup>\*1</sup>, 能勢 正仁<sup>\*2</sup>,  
松岡 彩子<sup>\*3</sup>, 寺本 万里子<sup>\*2</sup>, 今城 峻<sup>\*2</sup>

## DC component of spacecraft-origin magnetic field noise at the Arase/MGF sensor: (1) Evaluation with Tsyganenko 89 model

Kazuhiro YAMAMOTO<sup>\*1</sup>, Satoshi OIMATSU<sup>\*1</sup>, Masahito NOSE<sup>\*2</sup>, Ayako MATSUOKA<sup>\*3</sup>,  
Mariko TERAMOTO<sup>\*2</sup>, Shun IMAJO<sup>\*2</sup>

### ABSTRACT

We investigated the difference between the magnetic field observed by the Arase spacecraft and the Tsyganenko 89 model field ( $\Delta B$ ) during geomagnetic quiet period to determine the DC component of spacecraft-origin magnetic field noise at the position of Magnetic Field Experiment (MGF) onboard the Arase spacecraft. The median value of the Z-component of  $\Delta B$  in the Despun Sun sector Inertia (DSI) coordinates is very small (-0.6 nT); therefore, MGF has a good magnetic field cleanness and is well-calibrated. We also found that the Z-component of the magnetic field in the SM coordinate system observed by Arase is usually larger than that of the model field by  $\sim 3$  nT. The difference between time periods for the data used in this study and for the data to create the Tsyganenko 89 model may cause the discrepancy.

**Keywords:** ERG Project, Arase, MGF, offset, in-flight calibration

### 1. INTRODUCTION

The Arase spacecraft measures three dimensional velocity distributions of electrons and ions with a wide energy range to study wave-particle interactions. The accurate measurement of the electromagnetic field is important for this objective. The sensitivity and offset of Magnetic Field Experiment (MGF) onboard the Arase have already been evaluated in the ground calibration (Teramoto et al., 2017<sup>1)</sup>; Matsuoka et al., 2018<sup>2)</sup>). It was found that the magnetic field offset depends on temperature and its variation between -20 and 30 °C is less than 5 nT, which meets a requirement for MGF measurement of the magnetic field strength (Teramoto et al., 2017<sup>1)</sup>). Although the MGF instrument is equipped at the end of 5-m MAST to minimize contamination by spacecraft-origin magnetic field noises, the contamination during the satellite operation is not yet evaluated. In addition, in-flight temperature drift of the offset and inaccuracy of spacecraft attitude also cause some errors in magnetic field measurement.

The MGF is a fluxgate magnetometer composed of three orthogonal sensor elements. The X and Y elements are almost perpendicular to the spin axis of the spacecraft. The in-flight offsets and the stray field for X and Y elements can be determined from a sinusoidal waveform of the magnetic field due to the spin of the spacecraft. If the Earth's main field do not vary significantly in one spacecraft rotation ( $\sim 7.98$  s), the magnetic field measured by X/Y element will oscillate between  $B_0 \cos\theta + B_{Noise}$  and  $-B_0 \cos\theta + B_{Noise}$ , where  $B_0$  is the background magnetic field,  $\theta$  is an angle between  $B_0$  and the direction of the X/Y element, and  $B_{Noise}$  is the artificial magnetic noises including the magnetic field offset and the spacecraft-origin magnetic field noise. Thus the DC components of the magnetic field variation reflect these noises. This evaluation of the noises is performed in the process of the scientific data creation, and the noises for X and Y elements are corrected.

doi: 10.20637/JAXA-RR-18-005E/0004

\* Received October 8, 2018

<sup>\*1</sup> Graduate School of Science, Kyoto University

<sup>\*2</sup> Institute for Space-Earth Environmental Research, Nagoya University

<sup>\*3</sup> Department of Solar System Science, Institute of Space and Astronautical Science

Regarding the Z element, however, we cannot evaluate the noises in the same method, because the Z element almost directs to the spin axis. Since the temperature used for calibration of offset of the Z element is fixed at specific temperature, there is also an estimation error of the offset for the Z element. In this study, therefore, we statistically compare the magnetic field observed by the Z element with the Tsyganenko 89 (T89) model field (Tsyganenko, 1989<sup>3)</sup>) during geomagnetic quiet period, and evaluate the spacecraft-origin magnetic field noise and the estimation error of the offset on the Z element measurement.

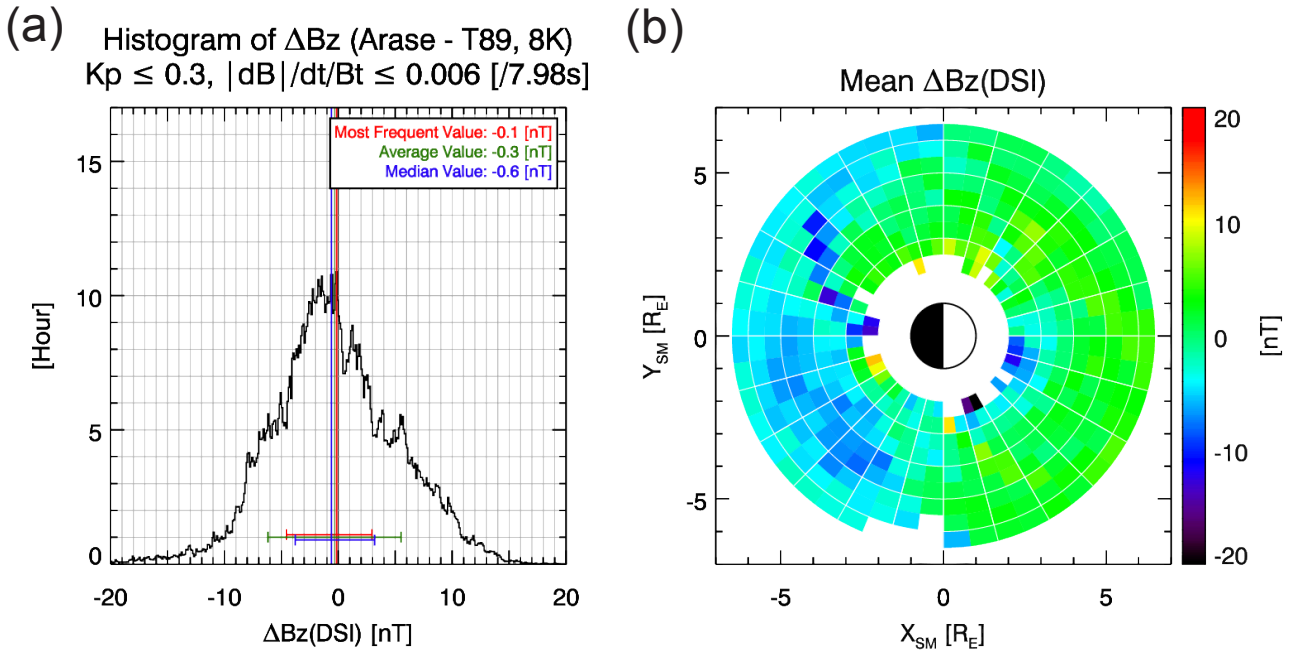


**Figure 1** (a) Histogram of the difference of  $B_{Z,DSI}$  between the Arase/MGF observation and the T89 model field. The vertical lines represent the most frequent value (red), the average value (green), and the median value (blue). The horizontal error bars show the full width of the half maximum (red), the standard deviation (green), and the first and third quartiles (blue). (b) R-MLT distribution of the averaged  $\Delta B_{Z,DSI}$  in the SM coordinate system.

## 2. ANALYSIS

### 2.1. Data Selection

We used the spin-averaged magnetic field data (v01.01) obtained by MGF from 23rd March 2017 to 30th April 2018. In this version, the data are calibrated for the sensitivity of MGF sensor using the temperature on the orbit, and for the miss alignment due to the twisting MAST. The offset of the Z element is estimated at a specific temperature from the results of the ground calibration, and the offset is subtracted from observed values.

We analyzed the data during geomagnetic quiet period to avoid a large difference between the observed magnetic field and the model field ( $\Delta B$ ) due to natural signals like dipolarization during substorms. The quiet periods were defined as intervals when the Kp index was 0o or 0+. We found about 1320 hours (55 days) of such period.

The MGF instrument has two dynamic ranges:  $\pm 8,000$  nT range and  $\pm 60,000$  nT range. MGF measures the magnetic field with  $\pm 60,000$  nT dynamic range near the Earth, but we excluded the  $\pm 60,000$  nT range data from our analysis because the determination error of the absolute sensitivity for the  $\pm 60,000$  nT range is too large (0.1 %) to evaluate the relatively small magnetic field noises. We imposed another criterion:  $\Delta B_{1-spin}/Bt < 0.006$ , where  $\Delta B_{1-spin}$  is the magnetic field variation in one spin period and  $Bt$  is the total intensity of the magnetic field. This is because  $|\Delta B|$  rapidly increases when  $\Delta B_{1-spin}/Bt$  is greater than 0.006.

From 1st October 2017 to 3rd November 2017, the algorithm for changing the dynamic range did not work well. Hence we did not examine this data period. Spike noises sometimes appear in the magnetic field data, and we removed them before the analysis.

## 2.2. Comparison with Tsyganenko 89 Model

After choosing the data during the geomagnetic quiet period, we calculated the model field values by using the T89 model. In the calculation, the Kp index was fixed at  $K_p = 0$  to express the ground state of the magnetosphere. We compared the observed magnetic field with the model field in the Despun Sun sector Inertia (DSI) coordinate system. In this coordinate system, Z axis ( $Z_{DSI}$ ) almost directs to the spin axis. Since the angle between  $Z_{DSI}$  and the spin axis is less than 1 degree, we can consider the Z-component of the magnetic field in the DSI coordinates ( $B_{Z,DSI}$ ) as the magnetic field observed by the Z sensor element. Our final goal is to evaluate the difference in  $B_{Z,DSI}$  between the spacecraft observation and the T89 model field ( $\Delta B_{Z,DSI}$ ).

The Arase spacecraft has an apogee altitude of  $\sim 32,000$  km and a perigee altitude of  $\sim 440$  km (Miyoshi et al., 2018<sup>4</sup>). Since Arase's apogee precesses 270 degree per year, we can examine  $\Delta B_{Z,DSI}$  at various radial distances (R) and magnetic local time (MLT). Arase's observation covers almost all MLT during the data period used in this study.

## 3. RESULTS

### 3.1. Histogram and R-MLT Distribution of the $\Delta B_{Z,DSI}$

Figure 1a shows the histogram of  $\Delta B_{Z,DSI}$  for the selected data period. Note that this histogram is strongly biased by the values around the apogee of Arase, because Arase was launched into elliptical orbit and the spacecraft spends much time around the apogee. Since the magnetic field noise originated from spacecraft should not vary with radial distances or MLT, it is appropriate for evaluation of the noise to use all period of the data. The most frequent value of  $\Delta B_{Z,DSI}$  is  $-0.1$  nT, the average value is  $-0.3$  nT, and the median value is  $-0.6$  nT. These values are much smaller than the offset of Z sensor element determined in the ground calibration (from  $-10$  to  $-13$  nT, Teramoto et al., 2017<sup>1</sup>). The histogram shows variance that may be created by weak geomagnetic disturbance. It seems that there are some local peaks around the maximum of the occurrence frequency in the histogram. Thus the median value is better than the other values to evaluate the noises. Figure 1b shows the radial distance vs MLT distribution of  $\Delta B_{Z,DSI}$  in a XY plane of the SM coordinate system. We found that  $\Delta B_{Z,DSI}$  depends on MLT; that is,  $\Delta B_{Z,DSI}$  is positive on the dayside while it is negative on the nightside.

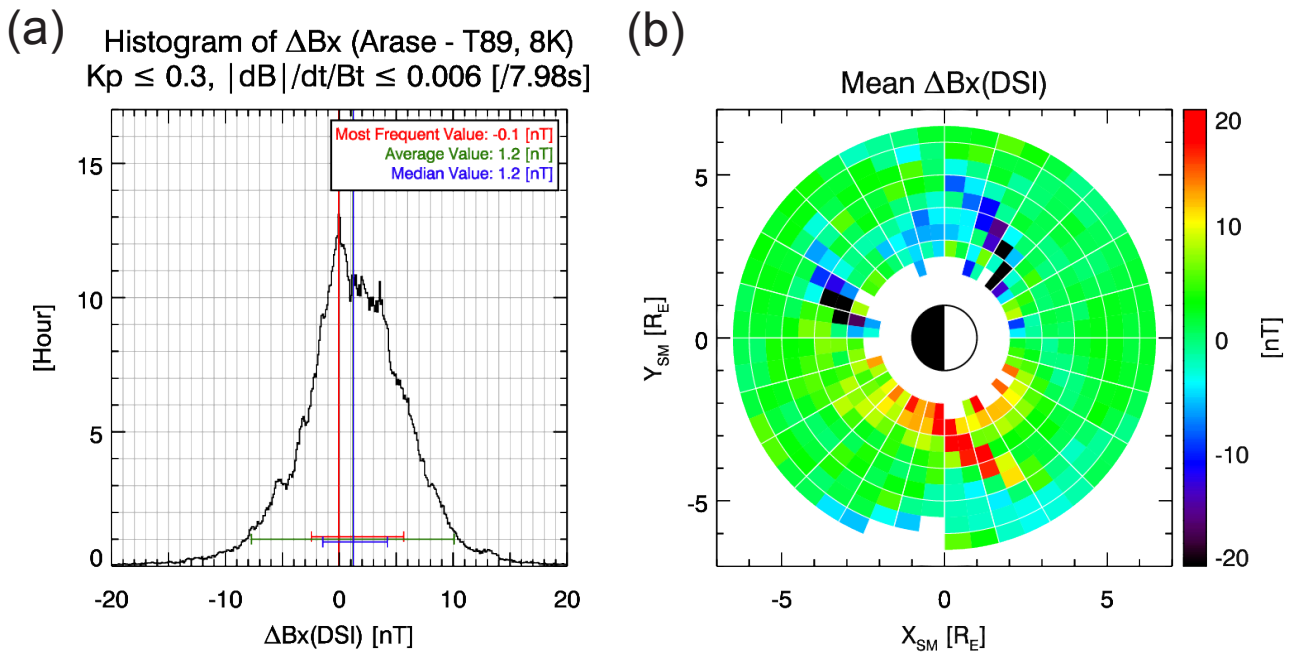


**Figure 2** (a) Same as Figure 1a but for  $\Delta B_{X,DSI}$ . (b) Same as Figure 1b but for  $\Delta B_{X,DSI}$ .

### 3.2. Histogram and R-MLT Distribution of the $\Delta B_{X,DSI}$ and $\Delta B_{Y,DSI}$

We also examined the differences between the observed magnetic field and the model field for X and Y components in the DSI coordinate system ( $\Delta B_{X,DSI}$  and  $\Delta B_{Y,DSI}$ ). The results are shown in Figures 2 and 3. As for  $\Delta B_{X,DSI}$ , the median value is slightly large (+1.2 nT) and variance of  $\Delta B_{X,DSI}$  seems more small than that of  $\Delta B_{Z,DSI}$ .  $\Delta B_{X,DSI}$  has no clear radial or local time dependence, and is usually positive (Figure 2b). The  $\Delta B_{Y,DSI}$  is the largest among the three components. The median value is 3.1 nT and the histogram has large variance (Figure 3a).  $\Delta B_{Y,DSI}$  also has no radial or local time dependence as shown in Figure 3b.

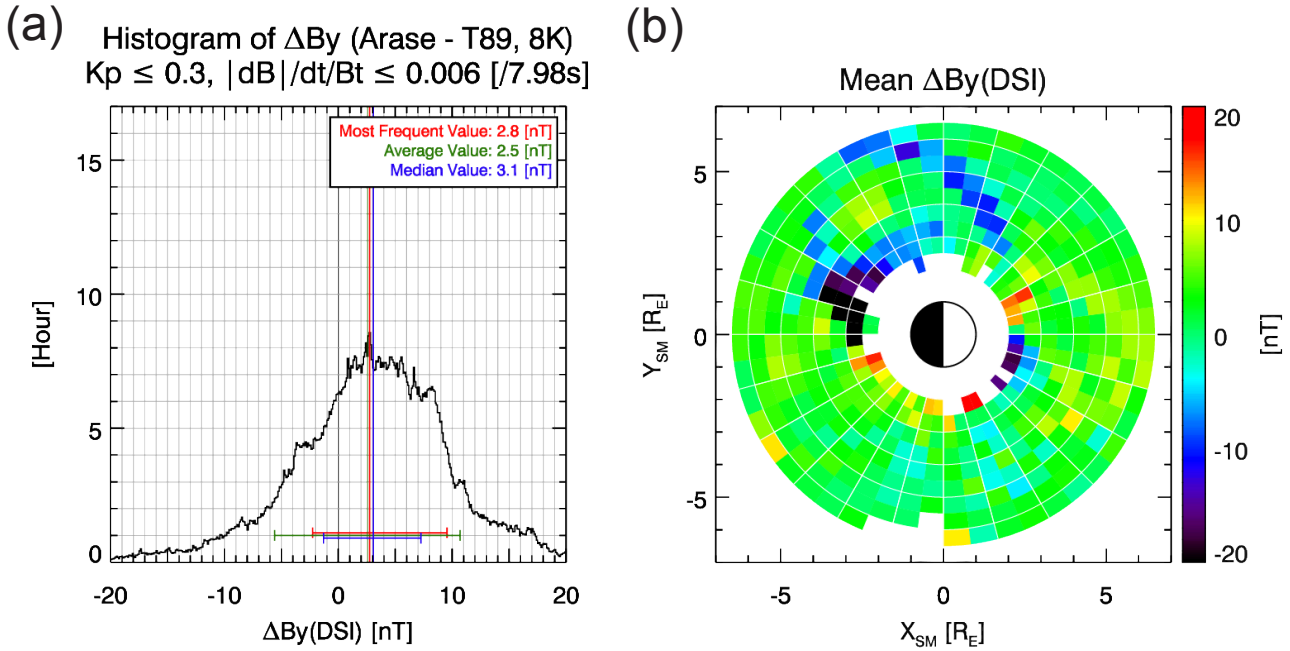


**Figure 3** (a) Same as Figure 1a but for  $\Delta B_{Y,DSI}$ . (b) Same as Figure 1b but for  $\Delta B_{Y,DSI}$ .

## 4. SUMMARY and DISCUSSION

### 4.1. Spacecraft-origin Noise and Estimation Error of the Offset in the Z Sensor Element

We compared the magnetic field observed by the Arase with the T89 model in the DSI coordinates during geomagnetic quiet period, and the result is summarized in Table 1. We cannot distinguish if these differences are caused by estimation errors of the sensor offset, the DC component of the spacecraft-origin magnetic field noise or the inaccuracy of the T89 model, because observational errors due to these factors can have similar values as discussed below. According to Teramoto et al. (2017)<sup>1)</sup>, the temperature drift of the offset for the Z element sensor is  $-0.1 \text{ nT}/^\circ\text{C}$  around  $0^\circ\text{C}$ . Therefore, the estimation error of the offset can be comparable to  $|\Delta B_{Z,DSI}|$  for different temperatures between in the offset estimation and in flight. The spacecraft-origin magnetic field noise at the tip of the MAST has been simulated by Matsuoka et al. (2017)<sup>2)</sup>, and they found that the turned-off spacecraft creates the spacecraft-origin noise by 0.18 nT. This value is also comparable to  $|\Delta B_{Z,DSI}|$ . The inaccuracy of the T89 model during the quiet period may be less than  $\sim 1 \text{ nT}$  and can contribute to  $\Delta B_{Z,DSI}$ . Nevertheless, the total influence of the artificial noises on the magnetic field measurement by the Z element may be very small (within  $\pm 1 \text{ nT}$ ) and the MGF sensor measures the magnetic field with high accuracy.

The clear MLT dependence of  $\Delta B_{Z,DSI}$  can be attributed to the inaccuracy of the MGF sensitivity or the T89 model, because the estimation error of the offset and the spacecraft-origin magnetic field noise should be independent on MLT. As a definition of the DSI coordinates,  $Z_{DSI}$  roughly directs to tailward. Since the Arase stays in the northern hemisphere for longer time than in the southern hemisphere (not shown), the positive  $\Delta B_{Z,DSI}$  on the dayside and the negative one on the nightside imply that the main field is stronger than that assumed in the T89 model. The error in the sensitivity is too small (0.06% for  $\pm 8,000 \text{ nT}$  range) to explain the large differences ( $> 1 \text{ nT}$ ). Therefore, we consider that the T89 model may underestimate the main field.

**Table 1** Differences between the magnetic field observed by the Arase spacecraft and the T89 model field in the DSI coordinate system during geomagnetic quiet period

	Most Frequent Value [nT]	Average Value [nT]	Median Value [nT]
$\Delta B_{X,DSI}$	-0.1	1.2	1.2
$\Delta B_{Y,DSI}$	2.8	2.5	3.1
$\Delta B_{Z,DSI}$	-0.1	-0.3	-0.6

#### 4.2. Interpretation of the large $\Delta B_{Y,DSI}$

As shown in Table 1,  $\Delta B_{Y,DSI}$  is the largest among the three components. To understand the reason for the large difference in  $B_{Y,DSI}$ , we investigated the direction of  $Y_{DSI}$  in the SM coordinates. Figure 4 shows the dwelling time of Arase as well as the three components of the unit vector along the  $Y_{DSI}$  axis in the SM coordinates. We can see that the  $Y_{DSI}$  axis approximately directs to the  $Z_{SM}$  axis except for the dusk sector. Therefore, the large  $\Delta B_{Y,DSI}$  may be due to the underestimation of the magnetic field in  $Z_{SM}$  ( $B_{Z,SM}$ ) by the T89 model. The magnetic field observed by Arase is closer to the dipole field than the model field.

Some possible reasons for the underestimation of  $B_{Z,SM}$  can be considered. Since the Arase's data period covers only the declining phase of the solar activity or the solar minimum, the magnetopause current may be weaker than that assumed in the T89 model. Thus the magnetic field induced by the magnetopause current along the main field should be small, and the main field will be larger than that expected in the T89 model. The other possible reason is the secular variation of the main field. Since the T89 model was coded about 30 years ago, the model field assumes stronger internal magnetic field than the data period used in this study. This may causes some errors in the estimation of parameters for an external field induced by magnetospheric current system.

DSI Dir. in SM Coord., 8k nT Range, 23 Mar. 2017 - 30 Apr. 2018  
 $K_p \leq 0.3$ ,  $|dB|/dt/Bt \leq 0.006$  [7.98s]

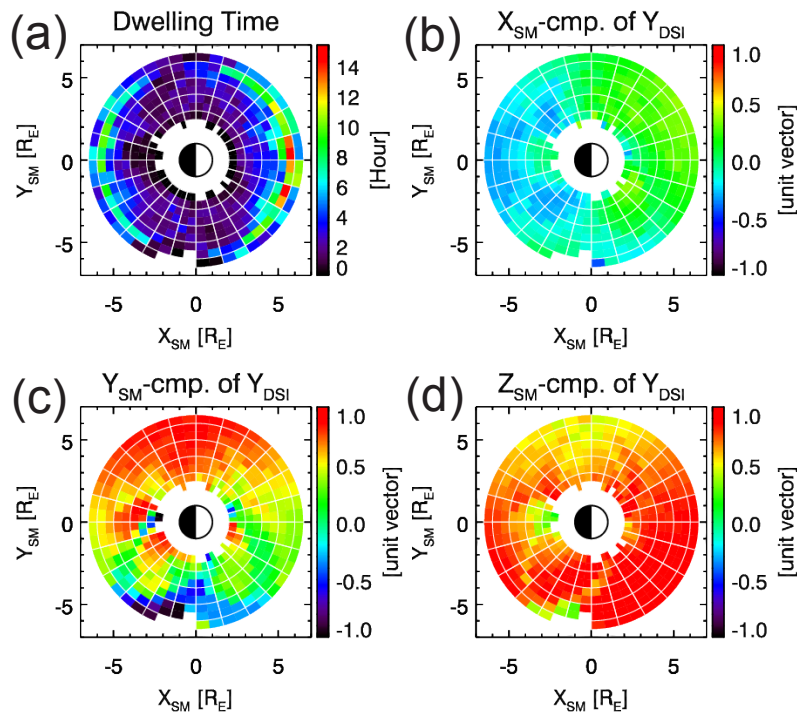


**Figure 4** (a) Dwelling time of the Arase spacecraft in XY plane of the SM coordinates. (b) X-component of the unit vector of  $Y_{DSI}$  axis. (c) Y-component of the unit vector of  $Y_{DSI}$  axis. (d) Z-component of the unit vector of  $Y_{DSI}$  axis.

## ACKNOWLEDGEMENTS

The MGF data used in this study (v01.01) were provided by ERG Science Center (<https://ergsc.isee.nagoya-u.ac.jp/data/ergsc/satellite/erg/mgf/>). The Kp index was provided by GeoForschungsZentrum (GFZ) Potsdam and was obtained from Kyoto University (<http://wdc.kugi.kyoto-u.ac.jp/kp/index-j.html>). This study is supported by Japan Society for the Promotion of Science (JSPS), Grant-in-Aid for Scientific Research (B) (grant 16H04057), Challenging Research (Pioneering) (grant 17K18804) and Grant-in-Aid for Specially Promoted Research (grant 16H06286).

## REFERENCES

- <sup>1)</sup> Teramoto M, Matsuoka A, Nomura R (2017) Ground calibration experiments of Magnetic field experiment on the ERG satellite (Japanese). *JAXA Research and Development Memorandum* JAXA-RM-16-003
- <sup>2)</sup> Matsuoka, A., Teramoto, M., Nomura, R., Nosé, M., Fujimoto, A., Tanaka, Y., Shinohara, M., Nagatsuma, T., Shiokawa, K., Obana, Y. and Miyoshi, Y. (2018). The ARASE (ERG) magnetic field investigation. *Earth, Planets and Space*, 70(1), 43.
- <sup>3)</sup> Tsyganenko, N. A. (1989). A magnetospheric magnetic field model with a warped tail current sheet. *Planetary and Space Science*, 37(1), 5-20.
- <sup>4)</sup> Miyoshi, Y., I. Shinohara, T. Takashima, K. Asamura, N. Higashio, T. Mitani, S. Kasahara, S. Yokota, Y. Kazama, S.-Y. Wang, S. W. Tam, P. T. P Ho, Y. Kasahara, Y. Kasaba, S. Yagitani, A. Matsuoka, H. Kojima, H. Katoh, K. Shiokawa, K. Seki (2018), Geospace Exploration Project ERG, *Earth, Planets and Space*, doi:10.1186/s40623-018-0862-0.